

Properties of holons in the Quantum Dimer Model

Didier Poilblanc¹

¹ *Laboratoire de Physique Théorique, CNRS & Université de Toulouse, F-31062 Toulouse, France*
(Dated: November 9, 2018)

I introduce a doped two-dimensional quantum dimer model describing a doped Mott insulator and retaining the original Fermi statistics of the electrons. This model shows a rich phase diagram including a *d*-wave hole-pair unconventional superconductor at small enough doping and a bosonic superfluid at large doping. The hole kinetic energy is shown to favor binding of topological defects to the bare fermionic holons turning them into bosons, in agreement with arguments based on RVB wave-functions. Results are discussed in the context of cuprates superconductors.

PACS numbers: 75.10.Jm, 05.50.+q, 05.30.-d

The discovery of high temperature superconductivity in copper oxides triggered unprecedented efforts to understand the role of strong correlations in electronic systems. In Anderson's milestone paper [1], the "mother" correlated insulator, on top of which superconductivity emerges under doping, was proposed as a Resonating Valence Bond (RVB) state where localized electrons are paired up into singlet (bond) dimers due to antiferromagnetic (AF) exchange. Here, a substantial energy is gained from quantum resonance between different (short-range) dimer coverings. Re-formulating these ideas [2] at the Hamiltonian level, Rokhsar and Kivelson constructed a Quantum Dimer Model (QDM) involving orthogonal dimer coverings and local dimer flips [3] (see Fig. 1(a)), aimed to capture the physics of systems that possess a spin (pseudo-) gap. Surprisingly, the QDM proved also to be relevant in a variety of distinct fields such as e.g. frustrated Ising models [4], spin-orbital models [5] or superconducting junction arrays [6]. Although the ground state (GS) of the QDM on the square lattice is a Valence Bond Crystal (VBC) breaking lattice symmetry [7], finite doping is expected to melt the crystal. In that respect, the doped QDM is of great interest since potentially more tractable than microscopic *t*-*J* or Hubbard models while effectively retaining their basic physical processes (spin exchange and hole hopping).

The exact nature of holons, the charged spinless excitations of the doped RVB state, has been debated over the last two decades. In particular, their statistics is still unclear. Earlier work based on a variational RVB wave-function [8] suggested that hole excitations are (weakly interacting) *fermions*. Such a conclusion, although only justified for small enough kinetic energy, was reproduced in the context of the doped QDM [9]. Furthermore, it was argued [9] that the holon statistics should in fact be dictated by energetics considerations and that, under some circumstances, a holon could bind to a "vortex", (see e.g. Ref. 8 for a simple definition) leading to a *bosonic* composite. Z_2 gauge theories have recently brought powerful new tools [10] to describe such phenomena. However, a more quantitative large-scale numerical investigation of the microscopic doped QDM is clearly

needed. In this Letter, I perform such a program using Exact Diagonalizations (ED) of periodic 6×6 and 8×8 clusters [11] and propose a semi-quantitative phase diagram. In contrast to previous investigations of doped QDM's [12] with non-positive off-diagonal matrix elements (named "Frobenius" QDM's), I consider here the *non-Frobenius* doped QDM which incorporates the Fermi statistics [13] of the original electrons. Major differences in the phase diagrams shown in Fig. 2 are observed and discussed in the text. Of particular interest are: (a) a new unconventional *d*-wave superconducting phase (with possible lattice symmetry breaking) and (ii) a spectacular change of the hole statistics, from Fermi to Bose, by increasing doping or kinetic energy.

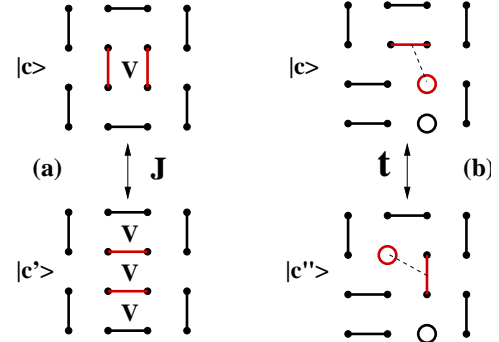


FIG. 1: (color online) Dimer flip (a) and holon hopping (b) in the QDM.

The non-Frobenius doped QDM model.—Following Ref. [3] and recent investigations [12], I start with the quantum hard-core dimer-gas on the two-dimensional square lattice defined by the Hamiltonian:

$$H = V \sum_c N_c |c\rangle \langle c| - J \sum_{(c,c')} |c'\rangle \langle c| - t \sum_{(c,c'')} |c''\rangle \langle c|$$

where the sum on (c) runs over all dimer coverings (containing a fixed amount of N_h vacant sites), N_c is the number of flippable plaquettes, the sum on (c', c) runs over all configurations $|c\rangle$ and $|c'\rangle$ that differ by a single plaquette dimer flip, and the sum on (c'', c) runs

over all configurations $|c\rangle$ and $|c''\rangle$ that differ by a single hole (or vacant site) hopping along a plaquette diagonal as pictured in Fig. 1. In this formulation, *bare* holons (i.e the moving vacancies) have Bose statistics. Since the system is originally composed of electrons of Fermi statistics, a faithful description should then assume that dimer configurations (with vacancies) are created by sets of (spatially symmetric) dimer operators expressed in the *fermionic* representation as e.g. in Refs. [2, 9], i.e. $d_{ij}^\dagger = \frac{1}{\sqrt{2}}(f_{i\uparrow}^\dagger f_{j\downarrow}^\dagger + f_{j\uparrow}^\dagger f_{i\downarrow}^\dagger)$ where $f_{i\sigma}^\dagger$ creates an electron of spin σ and i and j are neighboring sites. The original AF bond couplings yield then, in the QDM language, $J < 0$ and hence a *non-Frobenius* Hamiltonian with positive $-J = |J|$ off-diagonal matrix elements. Note that a bosonic convention for the dimers can equally well be used as will be discussed later on. So far the sign of t is not specified [15]. Phase diagrams (Fig. 2) are investigated as a function of $V/|J|$ and $|t/J|$.

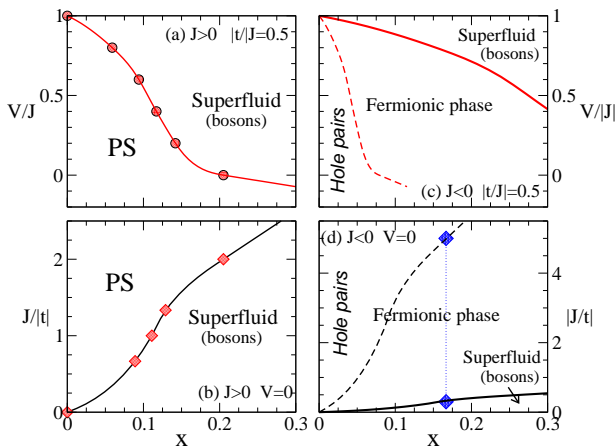


FIG. 2: (color online) Phase diagram of the doped QDM's versus doping (x) and $V/|J|$ (a,c) or $|t/J|$ (b,d). The Frobenius (a,b) and non-Frobenius (c,d) cases labelled on the plots as $J > 0$ and $J < 0$, respectively, (see text) are compared. The $x = 0$ insulator has VBC order. The symbols in (a,b) [resp. (d)] are obtained from the data of Fig. 3 [resp. Fig. 4].

About Phase Separation—On finite clusters, Phase Separation (PS) is signaled by a negative compressibility i.e. the local curvature of the energy vs doping $e(x)$ curve. In that case, the equilibrium hole densities of the two-component mixture can be obtained via a standard *Maxwell construction* as for an ordinary liquid-gas first-order transition. Using such a procedure one shows that the Frobenius QDM (i.e. with $J > 0$) phase separates at small doping [12]. The ED results for both signs of J are compared in Fig. 3; while for $J > 0$ the $x \rightarrow 0$ curvature of $e(x)$ is always negative, it is always positive for $J < 0$, even for small $|t/J|$ ratios. This shows that the two models behave quite differently in the immediate vicinity of the $x = 0$ axis as can already be noticed on their respective phase diagrams (Fig. 2) : (i) PS for

$J > 0$ (consistently with the data of Ref. 12 obtained for smaller $|t/J|$ and closer to the RK point $V/J = 1$) and (ii) a homogeneous phase (to be identified next) in the non-Frobenius case. In the latter case of most interest here, I find a very linear behavior of $e(x)$ at finite doping evolving into a region of negative curvature as soon as $|t/J| > 0.5$ suggesting that some form of PS might occur at *finite* doping.

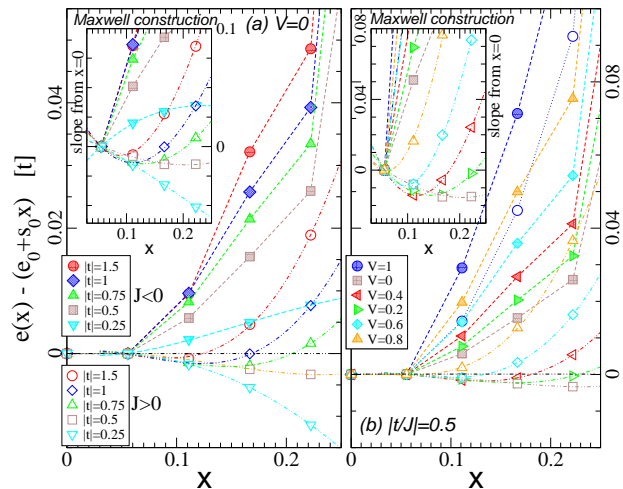


FIG. 3: (color online) On-site GS energy (per site) vs doping calculated on a 6×6 cluster. Full (open) symbols are used for the non-Frobenius (Frobenius) QDM labelled as $J < 0$ ($J > 0$). The linear behavior at $x \rightarrow 0$ has been subtracted for convenience. (a) $V = 0$ and different values of $|t|$; (b) $|t/J| = 0.5$ and different values of V (all in units of $|J| = 1$). Insets: mean-slopes between $x = 0$ and doping x plotted vs x . For $J > 0$, a polynomial fit gives a minimum at x_c providing the range $[0, x_c]$ of PS (Maxwell construction) reported in Fig. 2(a,b). For $J < 0$ no minimum at finite x is seen.

Melting of VBC order—How does the $x = 0$ VBC order evolve under finite doping is of great interest. Although, unfortunately, no finite-size scaling is possible here [13], a comparison with the Frobenius model (for which large systems could be studied, see [12]) is very instructive. As shown in Fig. 4(a), the relevant $\mathbf{q} = (\pi, 0)$ dimer-dimer correlator, decreases rapidly with the hole kinetic energy. However, at small enough $|t/J|$, the magnitude of the structure factor for the non-Frobenius model is always, on our clusters, larger than the same quantity in the Frobenius model. Since the later was shown to remain finite in the thermodynamic limit [12], this strongly suggests that there is, also in the non-Frobenius model, a finite region in the vicinity of $x = 0$ where VBC order survives. Note however that this phase is *not* phase-separated as in the Frobenius case. Interestingly enough, Fig. 4(a) also reveals at larger $|t/J|$ a sudden drop of the structure factor that we shall attribute later on to a real transition.

The d-wave superconductor—Let us now refine the

characterization of the low doping phase in the non-Frobenius model. Two doped holes [14] are found to form a zero-momentum bound-state, of $d_{x^2-y^2}$ symmetry providing one chooses $t > 0$ [15]. This is revealed by the “quasi-particle” (QP) peak at the bottom of the two-hole spectral functions plotted in Fig. 5(a-f). The associated weight Z_{2h} vanishes when approaching the RK point, i.e. $V/|J| \rightarrow 1$, where VBC correlations become algebraic (Fig. 5(h)). This suggests that pairing is due to confinement by the VBC, at least at large length-scales. Incidentally, a few higher energy peaks with approximate $(\frac{V}{|J|} - 1)^{2/3}$ energy dependence can be associated to so-called “string resonances”, typical of confinement phenomena. Interestingly enough, I also observed that the $|t/J|$ -dependance of Z_{2h} (Fig. 5(g)), $Z_{2h} \sim |J/t|^\eta$, $\eta \leq 1$, is quite similar to the case of a two-hole pair propagating in a quantum AF [16]. Since PS does not occur in the vicinity of the $x = 0$ axis one then expects a d-wave hole-pair superconductor in some finite doping range (see Fig. 2(c,d)). One could even argue (see above) that, at sufficiently small doping, d-wave (pair) superconducting and VBC orders are likely to coexist, although VBC order is not required for superconductivity.

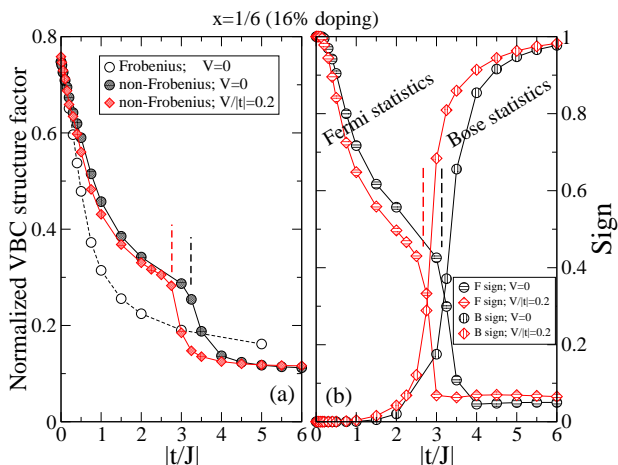


FIG. 4: (color online) (a) Columnar (i.e. $\mathbf{q} = (\pi, 0)$) VBC structure factor (normalized to its $x = 0$ value) versus $|t/J|$. (b) “Fermionic” and “bosonic” signs (as defined in text) vs $|t/J|$. (a) and (b) correspond to the non-Frobenius doped QDM with $V = 0$ (circles) and $V/|t| = 0.2$ (lozenges) at $x = 1/6$ (computed on a 6×6 cluster). In (a) additional data for the Frobenius case are shown for comparison. Vertical dotted segments give the approximate separations between the phases discussed in the text.

Holon statistics: Fermi vs Bose—Before turning to the investigation of the *actual* statistics of the holons, it is useful to mention briefly an alternative convention for the non-Frobenius QDM. Indeed, dimer operators can be represented in the usual bosonic representation $d_{i \rightarrow j}^\dagger = \frac{1}{\sqrt{2}}(b_{i\uparrow}^\dagger b_{j\downarrow}^\dagger - b_{i\downarrow}^\dagger b_{j\uparrow}^\dagger)$ in terms of boson creation

operator $b_{i\sigma}^\dagger$ carrying spin $\sigma = \pm \frac{1}{2}$, hence leading to a change of the sign of J , i.e. $J > 0$ (provided $d_{i \rightarrow j}^\dagger$ is oriented e.g. from the A to the B sublattice). However, to preserve the fermionic character of the original electron, the *bare* holon should be a fermion, meaning that one now keeps track of some fixed (arbitrary) ordering of the holons [17]. Obviously, the *actual* statistics of the holon is independent on the representation used.

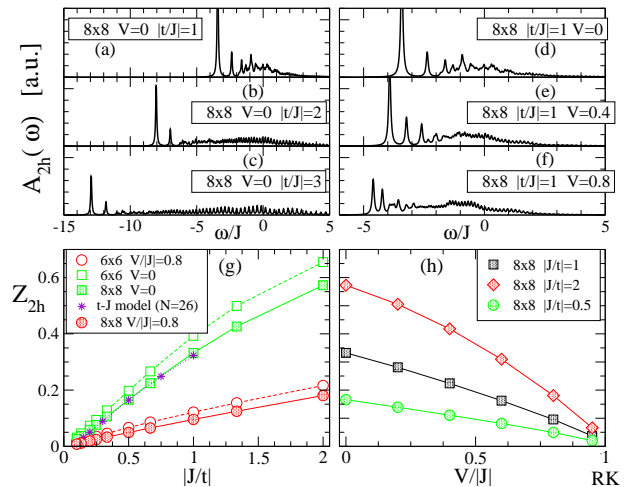


FIG. 5: (color online) (a-f) Spectral functions associated with the propagation of a $\mathbf{q} = (0, 0)$ d-wave pair of holes versus frequency ω (computed on a periodic 8×8 cluster) for fixed $V = 0$ (left) or $|t/J| = 1$ (right). The weight of the hole-pair QP peak (at the lowest energy edge) is plotted vs $|J/t|$ (g) and $V/|J|$ (h). Comparison with data on a 6×6 cluster in (g) suggests weak finite size effects. Data for the t-J model (stars) from Ref. 16 are also shown for comparison in (g). Note that “string resonances” can be seen above the QP peak in (a-f).

Motivated by [8] I now define “fermionic” (R=F) and “bosonic” (R=B) average signs as:

$$\text{Sign}_R = \sum_{\mathcal{H}_\alpha} \left| \sum_{c \in \mathcal{H}_\alpha} \langle \Psi_0^R | c \rangle \langle \Psi_0^R | c \rangle \right| / \sum_c |\langle \Psi_0^R | c \rangle|^2,$$

where the first sum is performed over all classes \mathcal{H}_α of configurations with fixed hole positions, the second sum runs over all dimer configurations within each class. The index “R” refers to one of the two (equivalent) representations of the non-Frobenius model (as discussed above) i.e. choosing *bare* holons with either Fermi (R=F) or Bose (R=B) statistics together with $J > 0$ (R=F) or $J < 0$ (R=B). Therefore, if holons truly behave as fermions (resp. holons) one expects $\text{Sign}_F \simeq 1$ (resp. $\text{Sign}_B \simeq 1$). Since a fermion (resp. boson) can be seen as a *bare* bosonic (resp. fermionic) holon bound to a vortex (or fluxoid) [8, 9, 10], one also expects simultaneously $\text{Sign}_B \simeq 0$ (resp. $\text{Sign}_F \simeq 0$) as the presence of vortices will “mess up” the equal sign of the weights of configurations with fixed hole positions. From the results displayed

in Fig. 4(b) one clearly identifies a clear and *simultaneous* rapid crossover of Sign_F and Sign_B signaling a change of statistics of the physical holons by binding/unbinding of vortices: at small (large) kinetic energy/doping, holon behaves as fermions (bosons) as argued from previous analysis [8, 9]. The separation line between these two regions have been estimated and reported in the phase diagrams of Fig. 2 (c,d) as a thick line. At large kinetic energy one expects the holons to Bose condensate giving rise to a charge-2e superfluid similar to the one of Refs. [10, 12] and Fig. 2 (a,b). The dotted lines of Fig. 2 (c,d) limit the area at small t or x where $\text{Sign}_F = 1$ within better than 5×10^{-3} , possibly connected to the superconducting and/or VBC phase.

Discussion and conclusion—To summarize, a non-Frobenius doped QDM retaining the Fermi statistics of the original electrons reveals a rich phase diagram. Holons doped in the VBC host are shown to behave as fermions at small enough doping and to pair up. This leads to a d-wave superconductor (possibly coexisting with VBC order) which shows striking similarities with the 2D t -J model. A key feature that permits the existence of this phase is the absence of PS in the immediate vicinity of the Mott insulator, in contrast to the Frobenius QDM [12]. At larger doping, with the disappearance of VBC order, holons behave as bosons and are expected to Bose condensate leading to a charge-2e superfluid [10, 12]. In this "statistics transmutation" the role of vortices (more specifically Z_2 vortices as described in Ref. [10]) is outlined. A complex behavior is also encountered in-between characterized by a rapid cross-over region where $\text{Sign}_F \sim \text{Sign}_B$ and some tendency towards PS. Identifying more precisely this cross-over is beyond the power of present-day computers but various hypothesis can be formulated. One scenario is a region of PS (i.e. *macroscopic* coexistence) of the two limiting phases which have been clearly identified in this work, as suggested by a slight negative curvature of $e(x)$ vs x in Fig. 3. Another alternative is that both (charged) fermionic and bosonic excitations coexist at intermediate doping in a way which might bear some resemblance with the "holon-hole superconductor" of Ref. [18] with, w.r.t. the large- x superfluid, additional low-energy excitations from paired holes. Incidentally, the observation of quantum oscillations attributed to some Fermi surface has been reported recently in cuprate superconductors [19]. In any case, the tendency towards phase separation leaves room for modulated/unidirectional structures (or stripes) once long-range Coulomb repulsion is included. This is of central interest since modulated structures have been seen in cuprate superconductors, e.g. in recent STM experiments [20].

Note that the present study has been realized on the square lattice where the undoped QDM has VBC order. It would also be of great interest to investigate the case of the triangular lattice where a deconfined RVB GS can

be realized in the Mott insulator [21].

I acknowledge hospitality from the Kavli Institute for Theoretical Physics while part of this work was done. This research was supported in part by the French Agence Nationale de la Recherche (ANR) under grant No. ANR-05-BLAN-043-01 and by the National Science Foundation under grant No. PHY05-51164. I also thank L. Balents, M. Fisher, S. Sachdev and T. Senthil for enlightening discussions.

-
- [1] P.W. Anderson, *Science* **235**, 1196 (1987).
 - [2] Large- N $Sp(2N)$ theories also include natural pairing of spins; see e.g. M. Vojta and S. Sachdev, *Phys. Rev. Lett.* **83**, 3916 (1999) and references therein.
 - [3] D.S. Rokhsar and S.A. Kivelson, *Phys. Rev. Lett.* **61**, 2376 (1988).
 - [4] R. Moessner and S. L. Sondhi, *Phys. Rev. B* **68**, 054405 (2003).
 - [5] F. Vernay, A. Ralko, F. Becca and F. Mila, *Phys. Rev. B* **74**, 054402 (2006).
 - [6] A.F. Albuquerque, H.G. Katzgraber, M. Troyer, G. Blatter, *Phys. Rev. B*, in press (2007).
 - [7] At $x = 0$ columnar, plaquette and mixed VBC are stabilized except at the RK point [3] ($V/|J| = 1$) which is critical on the square lattice. See e.g. O.F. Syljuasen, *Phys. Rev. B* **71**, 020401(R) (2005); A. Ralko, D. Poilblanc and R. Moessner, *Phys. Rev. Lett.*, in press. At $x = 0$ the sign of J is irrelevant.
 - [8] N. Read and B. Chakraborty, *Phys. Rev. B* **40** 7133 (1989); see also P. Lederer and Y. Takahashi, *Z. Phys. B* **71**, 311 (1988).
 - [9] S. Kivelson, *Phys. Rev. B* **39**, 259 (1989).
 - [10] T. Senthil and M.P.A. Fisher, *Phys. Rev. B* **62** 7850 (2000); see also L. Balents, M.P.A Fisher and C. Nayak, *Phys. Rev. B* **60**, 1654 (1999).
 - [11] All space group symmetries are used to block-diagonalize the hamitonian.
 - [12] A. Ralko, F. Mila and D. Poilblanc, *Phys. Rev. Lett.* **99** 127202 (2007); see also D. Poilblanc, F. Alet, F. Becca, A. Ralko, F. Trouselet and F. Mila, *Phys. Rev. B* **74**, 014437 (2006).
 - [13] When the Perron-Frobenius theorem (1908) does not hold the GS wavefunction acquires nodes precluding Quantum Monte Carlo studies ("minus sign problem").
 - [14] For $N_h = 2$ and 8×8 , there are 102 969 156 symmetrized states in the GS sector. The GS energy is $-22.336 584$ for $V = 0$ and $|J| = |t| = 1$.
 - [15] The gauge transformation performing $t \rightarrow -t$ interchanges quantum numbers (like orbital symmetry).
 - [16] D. Poilblanc, *Phys. Rev. B* **48**, 3368 (1993).
 - [17] The equivalence of the two representations has been checked numerically.
 - [18] R.K. Kaul, Y.B. Kim, S. Sachdev and T. Senthil, *Nature Physics*, **4**, 28 (2008); D. Poilblanc, *ibid* **16** (2008).
 - [19] N. Doiron-Leyraud et al., *Nature* **447**, 565 (2007).
 - [20] Y. Kohsaka et al., *Science* **315**, 1380 (2007) and references therein.
 - [21] A. Ralko, M. Ferrero, F. Becca, D. Ivanov, and F. Mila, *Phys. Rev. B* **71**, 224109 (2005).